Communications

Literature Survey on Diffusivities of Oxygen, Aluminum, and Vanadium in Alpha Titanium, Beta Titanium, and in Rutile

Z. LIU and G. WELSCH

A survey of diffusion data of interstitial oxygen and of the substitutional elements aluminum and vanadium is presented for alpha and beta titanium. It is based on a survey of literature. Oxygen is an important interstitial element in titanium alloys. Oxygen's large chemical affinity to titanium is indicated by Ti—O bond energy of 2.12 eV,[1] comparable to the Ti—Ti bond energy of 2.56 eV.[2] Oxygen is difficult to eliminate completely from titanium, and commercial titanium alloys usually contain from 0.10 to 0.20 wt pct oxygen. Oxygen significantly affects the mechanical properties of titanium alloys[1,3] and is sometimes used as an alloying element. The effects of oxygen on phase transformation,[4,5,6] Youngs modulus,[7,8] hardness,[9,10] fracture toughness,[11] and other mechanical properties[12] have been amply documented. Aluminum and vanadium are the most frequently used substitutional alloying elements. Aluminum is an alpha stabilizer and vanadium is a beta stabilizer.

The diffusion of oxygen, aluminum, and vanadium plays an important role in the establishment of phase morphologies during heat treatment and processing. The diffusivity of oxygen is also important for the homogenization of oxide films in powder metallurgical compacts, and it affects the thickness of the oxygen-rich alpha scale formed during treatments in oxidizing environment. There exist many investigations of the diffusivities of these elements. However, they are scattered over many journals over a period of more than 30 years. The objective of the present survey was to combine the essential information from these references into an overview for easy comparison.

Several methods have been used for oxygen diffusivity measurements, such as internal friction, oxidation, and evaluation of oxygen concentration gradients. For the diffusivities of aluminum and vanadium, the concentration gradient method has been commonly used. Diffusion distances have been measured by metallography, microhardness profile, microprobe analysis, and X-ray analysis, or were indicated by tracer atoms, such as V48.[13,14] The concentration gradient method uses a pair of metal samples of different alloy concentrations in contact with each other. After keeping them at a given temperature for a period of time, the concentration profile of the diffusing element can be measured to yield the diffusion coefficient. Based on several diffusion coefficient determinations at different temperatures, the pre-exponential frequency factor D_0 and the activation

energy Q of the temperature dependence of diffusivity,

$$D = D_0 \exp(-Q/RT),$$

can be obtained. The internal friction method has been used at relatively low temperatures to measure the diffusivity of oxygen. When a stress is applied to a sample along one direction, randomly distributed interstitial solute atoms will tend to move to a position of minimum local strain energy. This is the case whenever the solute atoms (or pairs or clusters of solute atoms) are surrounded by tetragonal strain field. Under oscillating stress condition an internal friction peak occurs at a temperature at which the successful jump frequency of interstitial atoms equals the oscillation frequency. The diffusion coefficient D at this temperature is related to the success jump frequency Γ by

$$D = \Gamma x^2/6$$

where x is the effective jump distance.[15–18] The oxidation method generates not only an oxide scale but also an oxygen concentration gradient in the metal substrate. When beta-Ti is oxidized at temperatures above the beta transus temperature, an alpha-Ti layer will form below the oxide scale. The boundary between the alpha layer and the beta base alloy will move inward as oxygen diffusion proceeds. The rate of movement of the alpha/beta interface depends on the oxygen transport rate through the alpha layer and permits evaluation of oxygen diffusivity in alpha-Ti. To determine the oxygen diffusivity in beta-Ti, the oxygen concentration gradient in the beta-phase must be measured directly.[19]

Table I shows the pre-exponential constants and activation energies of oxygen diffusion in alpha-Ti, determined by various methods. The pre-exponential constants and activation energies of aluminum diffusion in alpha-Ti are listed in Table II. The diffusion coefficients are plotted in Figure 1. The oxygen diffusion data, except those from internal friction, fall into a narrow band and are in good agreement with each other. The aluminum diffusion data are scattered. For line 1 of Al diffusivity, shown in Figure 1, high accuracy was not claimed by the author because only two data points over a limited temperature region (only 66 °C) had been obtained.[44] However, because of the scarcity of data it is not clear whether the other Al-data are more reliable. From intuition one would expect the Al-diffusivities to be less than those of oxygen.

Tables III, IV, and V list the pre-exponential constants and activation energies of diffusion of oxygen, aluminum, and vanadium, respectively, in beta-Ti. The data are plotted in Figure 2. At 1000 °C the diffusion coefficient of oxygen is about one order of magnitude higher than that of vanadium and about 1 to 3 orders of magnitudes higher than that of aluminum. Line 2 for oxygen appears to have an excessively high slope (activation energy). It is not clear why there are such large differences in the data for the diffusion coefficients of Al and V determined by various authors.

An abnormal temperature dependence of the diffusion data has sometimes been reported[54] for which Arrhenius plots of ln D vs $1/T$ do not give a single straight line, as would be the case for constant D_0 and Q. A curve of the effective diffusion coefficient D is based on two contributions at high and low temperatures, according to

Table I. The Pre-Exponential Constants and Activation Energies for Diffusion of Oxygen in Alpha Titanium

Ser. No.	Temp. (K)	D_0 (m^2/sec)		Q (kJ/mole)	Alloy	Method	Ref.
1	~723	0.4	$\times\ 10^{-4}$	201	Ti-3.5 at. pct O	int. fri.	20
2		1.8	$\times\ 10^{-7}$	150	Ti	int. fri.	21
3	~683	(0.5 to 1)	$\times\ 10^{-4}$	245 ± 10	Ti	int. fri.	22
4	~690	(0.5 to 1)	$\times\ 10^{-4}$	243 ± 10	Ti-0.3 at. pct O	int. fri.	22
5	~698	0.5	$\times\ 10^{-4}$	241 ± 10	Ti-0.6 at. pct O	int. fri.	22
6	~723	1	$\times\ 10^{-4}$	188 ± 21	Ti-2.0 at. pct O	int. fir.	23
7	~693	0.8	$\times\ 10^{-4}$	243 ± 13	Ti-(0.9 to 1.7) at. pct O	int. fri.	24
8	~728	1	$\times\ 10^{-4}$	203 ± 21	Ti	int. fri.	25
9	973 to 1123	5.08	$\times\ 10^{-7}$	140	Ti	conc. grad., MG & MH[a]	26
10	723 to 823	4.97	$\times\ 10^{-11}$ [b]	102[b]	Ti	conc. grad., AES[c]	27
11	1123 to 1273	3.20	$\times\ 10^{-2}$	259 ± 0.8	Ti	oxid.	28
12	1173 to 1573	8.9	$\times\ 10^{-4}$	220	Ti	oxid.	29
13	811 to 1089	6.2	$\times\ 10^{-5}$	203	Ti-6Al-2Sn-4Zr-2Mo	oxid.	30
14	1205 to 1415	7.78	$\times\ 10^{-5}$	203	Ti	oxid.	22
15	1023 to 1123	1.7	$\times\ 10^{-3}$	219	Ti-1.0 at. pct O	oxid.	31
16	923 to 1148	4.08	$\times\ 10^{-5}$	197	Ti	oxid.	32
17	973 to 1223	4.5	$\times\ 10^{-5}$	201	Ti	oxid.	33
18	1023 to 1173	2.15[b]		298[b]	Ti	oxid.	34
19	1088 to 1422	20.3		315	Ti	oxid., hardness	35
20	1088 to 1422	9.24	$\times\ 10^{-3}$	246	Ti-5Al-2.5Sn	oxid., hardness	35
21	1088 to 1422	7.49	$\times\ 10^{-3}$	232	Ti-4Al-4Mn	oxid., hardness	35
22	1023 to 1323	9.4	$\times\ 10^{-2}$	287	Ti	oxid., TGA[d]	36
23	523 to 1173	4.5	$\times\ 10^{-5}$	200 ± 30	Ti	oxid., SSA[e]	37 to 41
24	1023 to 1143	1.6	$\times\ 10^{-3}$	218	Ti	oxid., MH & XSA[f]	42
25		(7.8 to 160)	$\times\ 10^{-5}$	188 to 220	Ti	theor. estimate	43

(a) metallography and microhardness (c) Auger electron spectroscopy (e) stress-strain aging method
(b) derived from the diffusion data (d) thermogravimetric analysis (f) microhardness and X-ray structure analysis

Table II. The Pre-Exponential Constants and Activation Energies for Diffusion of Aluminum in Alpha Titanium

Ser. No.	Temp. (K)	D_0 (m^2/sec)	Q (kJ/mole)	Alloy	Method	Ref.
1	1107 to 1173	1.60×10^{-9}	99.2	Ti-10 at. pct Al	conc. grad.	44
2	833 to 921	9.59×10^{-10} [a]	92.5[a]	Ti	conc. grad., EMA[b]	45
3	973 to 1173	1.58×10^{-16}	77.0	Ti-2Al	conc. grad.	46
4	973 to 1173	8.70×10^{-17}	70.7	Ti-4.1Al	conc. grad.	46

(a) derived from the diffusion data
(b) electron microprobe analysis

Table III. The Pre-Exponential Constants and Activation Energies for Diffusion of Oxygen in Beta Titanium

Ser. No.	Temp. (K)	D_0 (m^2/sec)	Q (kJ/mole)	Alloy	Method	Ref.
1	1400 to 1620	8.3×10^{-6}	131 ± 8.4	Ti	conc. grad.	47
2	1173 to 1423	3.14	288	Ti	conc. grad.	26
3	1223 to 1423	6.3×10^{-5}	155	Ti	conc. grad., XSA[a]	48
4	1608 to 1848	2×10^{-6}	115 ± 17	Ti	conc. grad.	49
5	1223 to 1687	1.6×10^{-4}	202 ± 13	Ti	oxid.	50
6	1205 to 1415	3.30×10^{-2}	246	Ti	oxid.	19
7	1173 to 1323	9.34×10^{-7} [b]	151[b]	Ti	oxid.	34
8	1173 to 1423	1.4×10^{-5}	138	Ti	oxid.	31
9	1223 to 1403	4.5×10^{-5}	151	Ti	oxid., hard. & X SA[a]	42
10		2×10^{-6}	149	Ti-45Nb	theor. estimate	51

(a) X-ray structure analysis
(b) derived from the diffusion data

Table IV. The Pre-Exponential Constants and Activation Energies for Diffusion of Aluminum in Beta Titanium

Ser. No.	Temp. (K)	D_0 (m^2/sec)	Q (kJ/mole)	Alloy	Method	Ref.
1	1256 to 1523	1.4×10^{-9}	91.7 ± 15	Ti-2 at. pct Al	conc. grad.	44
2	1256 to 1523	9.0×10^{-9}	107 ± 20	Ti-12 at. pct Al	conc. grad.	44
3	1373 to 1523	1.09×10^{-10}	172	Ti-2.2 Al	conc. grad.	46
4	1373 to 1523	2.90×10^{-10}	180	Ti-4.55 Al	conc. grad.	46

Table V. The Pre-Exponential Constants and Activation Energies for Diffusion of Vanadium in Beta Titanium

Ser. No.	Temp. (K)	D_0 (m²/sec)	Q (kJ/mole)	Alloy	Method	Ref.
1	1173 to 1521	6.0×10^{-6}	166 ± 20	Ti-2 at. pct V	conc. grad.	44
2	1173 to 1273	1.37×10^{-8}	239[a]			
		3.10×10^{-8}	135[b]	Ti	conc. grad.	13
3	1173 to 1273	5.89×10^{-8}	170[a]			
		3.31×10^{-7}	157[b]	Ti	conc. grad.	14
4	1173 to 1473	3.55×10^{-8}	161[a]			
		3.98×10^{-7}	163[b]	Ti-10V	conc. grad.	14
5	1173 to 1473	1.29×10^{-4}	273[a]			
		7.00×10^{-7}	173[b]	Ti-20V	conc. grad.	14
6	1173 to 1273	1.31×10^{-12}	44.4[c]	Ti-15 at. pct V	conc. grad., XS[d]	52
7	1173 to 1273	1.10×10^{-14}	21.2[c]	Ti-20 at. pct V	conc. grad., XS[d]	52
8	1223 to 1783	1.24×10^{-8}	239[e]			
		4.46×10^{-12}	140[f]	Ti-0.01 at. pct V	conc. grad.	53

(a) D_{01} and Q_1, derived from the diffusion data   (c) derived from the diffusion data   (e) D_{01} and Q_1
(b) D_{02} and Q_2, derived from the diffusion data   (d) X-ray spectra   (f) D_{02} and Q_2
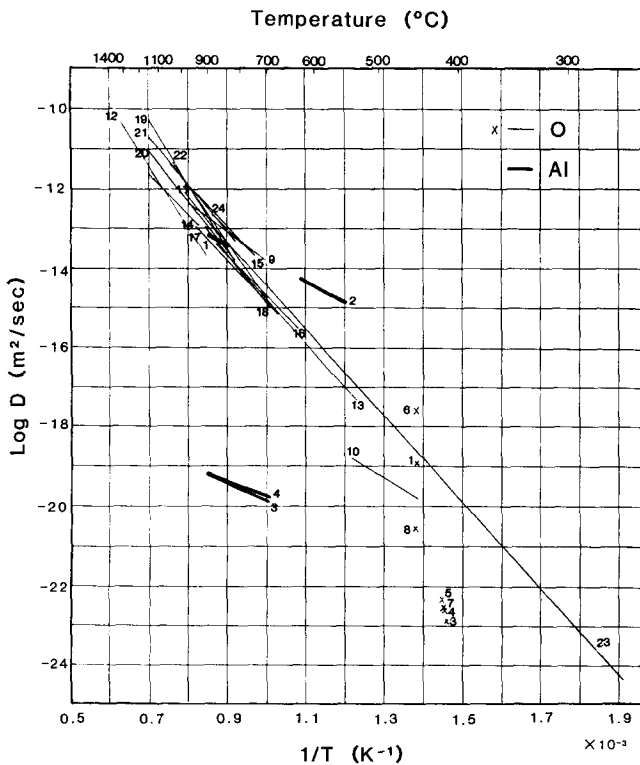

Fig. 1 — The diffusivities of oxygen and aluminum in alpha-Ti. The numbers in the plot correspond to the series numbers in Tables I and II.

$$D = D_{01} \exp(-Q_1/RT) + D_{02} \exp(-Q_2/RT).$$

D_{01} and Q_1 dominate at high temperatures, and D_{02} and Q_2 are dominant at low temperatures. Where such distinc-
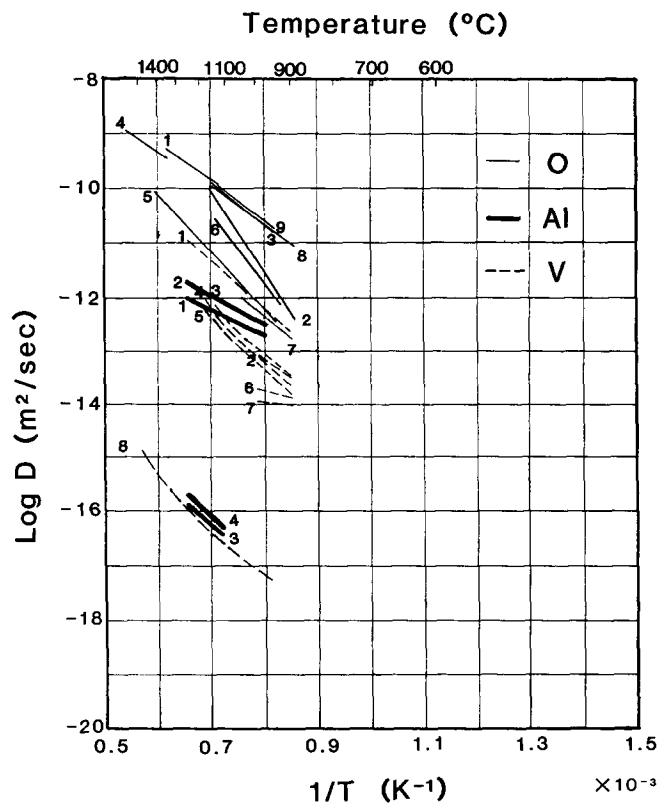

Fig. 2 — The diffusivities of oxygen, aluminum, and vanadium in beta-Ti. The numbers in the plot correspond to the series numbers in Tables III, IV, and V.

Table VI. The Pre-Exponential Constants and Activation Energies for Diffusion of Oxygen in Rutile

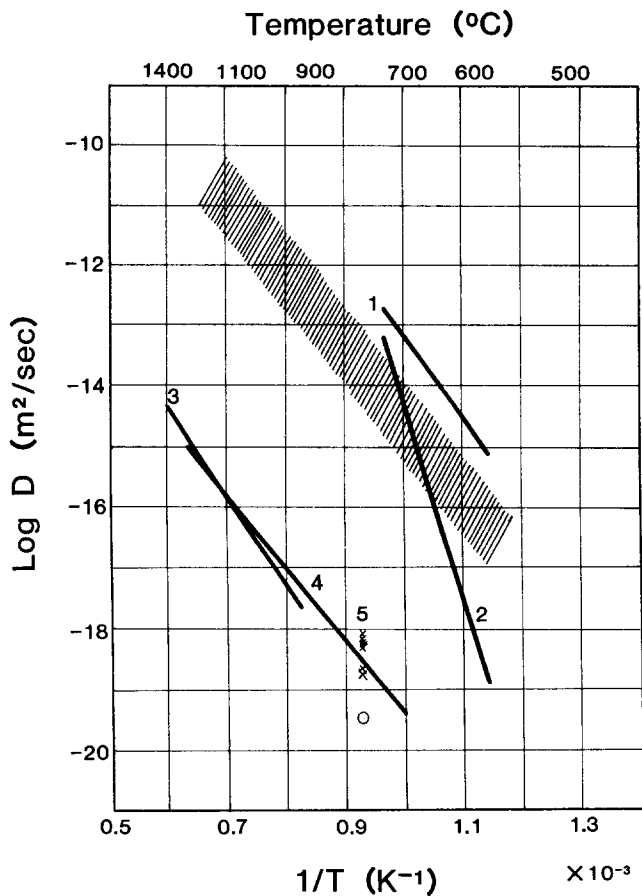| Ser. No.	Temp. (K)	D_0 (m²/sec)	Q (kJ/mole)	Material	Method	Ref.
1	866 to 1033	8.7×10^{-2}	232	oxide scale on Ti	oxid.	55
2	866 to 1033	2.69×10^{-2}	242.9	oxide scale on Ti-6Al-2Sn-4Zr-2Mo	oxid.	56
3	1233 to 1673	1.7×10^{-6}	276	oxide scale on Ti	resonance capture	57
4	983 to 1573	2.0×10^{-7}	251	TiO_2	isotope exchange	58
5	1079	only individual D's		oxide scale on Ti	isotope exchange	59

Temperature (°C)

Fig. 3 — The diffusivity of oxygen in rutile. The numbers in the plot correspond to the series numbers in Table VI. The crosses and the circle indicate the diffusivities along and perpendicular to the c-axis of rutile crystals.[59] For comparison, the diffusivity of oxygen in α-Ti is indicated by the hatched area.

tions have been made in the literature, they are indicated in Table V.

Table VI lists the pre-exponential constants and activation energies of diffusion of oxygen in rutile, TiO_2. The data are plotted in Figure 3. For comparison, the diffusivity of oxygen in α-Ti is indicated by the hatched area.

REFERENCES

1. H. Conrad: Prog. in Mat. Sci., 1981, vol. 26, p. 138.
2. A. Kant and B. Strauss: J. Chem. Phys., 1964, vol. 41, pp. 3806-08.
3. H. Margolin and J. P. Nielsen: Modern Materials, H. H. Hausner, ed., 1960, vol. 2, pp. 225-325.
4. J. C. Williams: Titanium Science and Technology, R. I. Jaffee and H. M. Burte, eds., Plenum Press, 1973, pp. 1454-58.
5. M. A. Nikhanorov and V. V. Latsh: Titanium and Titanium Alloys, J. C. Williams and A. F. Belov, eds., Plenum Press, 1976, p. 1655.
6. A. I. Kahveci and G. Welsch: Scripta Metall., 1986, vol. 20, pp. 1287-90.
7. H. Conrad: Prog. in Mat. Sci., 1981, vol. 26, p. 136.
8. G. Welsch and W. Bunk: Metall. Trans. A, 1982, vol. 13A, pp. 889-99.
9. R. I. Jaffee: Prog. in Metal Phys., 1958, vol. 7, p. 109.
10. Z. Liu and G. Welsch: Metall. Trans. A, 1988, vol. 19A, pp. 527-42.
11. M. J. Harrigan, M. P. Kaplan, and A. W. Sommer: Titanium and Titanium Source Book, ASM, Metals Park, OH, 1982, pp. 50-79.
12. R. I. Jaffee: Titanium '80 Science and Technology, H. Kimura and O. Izumi, eds., TMS-AIME, 1980, p. 53.

13. J. F. Murdock, T. S. Lundy, and E. E. Stansbury: Acta Metall., 1964, vol. 12, pp. 1033-39.
14. J. F. Murdock and C. J. McHargue: Acta Metall., 1968, vol. 16, pp. 493-500.
15. A. S. Nowick and B. S. Berry: Anelastic Relaxation in Crystalline Solids, Academic Press, New York, NY, 1972, p. 14.
16. P. Kofstad: High-Temperature Oxidation of Metals, John Wiley & Sons, Inc., New York, NY, 1966, p. 157.
17. J. L. Bocquet, G. Brebec, and Y. Limoge: in Physical Metallurgy, R. W. Cahn and P. Haasen, eds., North Holland Physical Pub., 1983, pp. 408-09.
18. D. A. Porter and K. E. Easterling: Phase Transformation in Metals and Alloys, von Nostrand Reinhold, 1987, pp. 63-65.
19. C. J. Rosa: Metall. Trans., 1970, vol. 1, pp. 2517-22.
20. J. N. Pratt, W. J. Bratina, and B. Chalmers: Acta Metall., 1954, vol. 2, pp. 203-08.
21. A. V. Revyakin: Izv. Akad. Nauk. SSSR, Otd. Tekhn. Nauk, Met. i Toplivo, 5 (1961), pp. 113-16, from P. Kofstad, High-Temperature Oxidation of Metals, John Wiley & Sons, Inc., New York, NY, 1966, Ref. 203.
22. D. R. Miller: Trans. TMS-AIME, 1962, vol. 224, pp. 275-81.
23. D. Gupta and S. Weinig: Acta Metall., 1962, vol. 10, pp. 292-98.
24. D. R. Miller and K. M. Browne: The Science, Technology and Application of Titanium, R. I. Jaffee and N. E. Promisel, eds., The Science, Pergamon Press, 1968, pp. 401-06.
25. K. M. Browne: Acta Metall., 1972, vol. 20, pp. 507-14.
26. W. P. Roe, H. R. Palmer, and W. R. Opie: Trans. ASM, 1960, vol. 52, pp. 191-200.
27. T. N. Wittberg, J. D. Wolf, R. G. Keil, and P. S. Wang: J. Vac. Sci. Technol. A, 1983, vol. A1(2), pp. 475-78.
28. J. Stringer: Acta Metall., 1960, vol. 8, pp. 758-66.
29. P. Kofstad: J. Less-Common Met., 1967, vol. 12, pp. 449-64.
30. C. E. Shamblen and T. K. Redden: The Science, Technology and Application of Titanium, R. I. Jaffee and N. E. Promisel, eds., The Science, Pergamon Press, 1968, pp. 199-208.
31. D. V. Ignatov, M. S. Model, L. F. Sokyriansky, and A. Ya. Shinyaev: Titanium Science and Technology, R. I. Jaffee and H. M. Burte, eds., Plenum Press, 1973, pp. 2535-44.
32. M. Dechamps and P. Lehr: J. Less-Common Met., 1977, vol. 56, pp. 193-207.
33. D. David, E. A. Garcia, G. Beranger, J. P. Bars, E. Etchessahar, and J. Debuigne: Titanium '80 Science and Technology, H. Kimura and O. Izumi, eds., TMS-AIME, 1980, pp. 537-47.
34. V. I. Tikhomirov and V. I. D'yachkov: Phys. Met. Metallogr., 1970, vol. 30, pp. 115-20.
35. J. E. Reynolds, H. R. Ogden, and R. I. Jaffee: Trans. ASM, 1957, vol. 49, pp. 280-99.
36. V. I. Tikhomirov and V. I. Dyachkov: Zh. Prikl. Khim., 1967, vol. 40, pp. 2405-13, from Diffusion Data, vol. 2, p. 308.
37. D. David, G. Beranger, and E. A. Garcia: J. Electrochem. Soc., 1983, vol. 130, pp. 1423-26.
38. D. David, E. A. Garcia, X. Lucas, and G. Beranger: J. Less-Common Met., 1979, vol. 65, pp. 51-69.
39. E. de Paula E. Silva: Thesis, University of Paris XI, Paris, France, 1972, from Ref. 37.
40. E. de Paula E. Silva, E. A. Garcia, and G. Beranger: "Journees d'Etude du Titane at de Ses Alliages", Nantes, 1973, from Ref. 37.
41. Y. A. Bertin: Thesis, Poitiers, 1979, from Ref. 37.
42. L. F. Sokiryanskiy, D. V. Ignatov, and A. Ya. Shinyaev: Phys. Met. Metallogr., 1969, vol. 28, pp. 103-08.
43. H. Conrad, M. Doner, and B. de Meester: Titanium Science and Technology, R. I. Jaffee and H. M. Burte, eds., Plenum Press, 1973, p. 970.
44. D. Goold: J. Inst. of Met., 1959-60, vol. 88, pp. 444-48.
45. J. Pouliquen, S. Offret, and J. de Fouquent: C. R. Acad. Sci., Paris, 1972, Serie C, vol. 274, pp. 1760-63.
46. K. Ouchi, Y. Iijima, and K. Hirano: Titanium '80 Science and Technology, H. Kimura and O. Izumi, eds., TMS-AIME, 1980, pp. 559-68.
47. F. Claisse and H. P. Koenig: Acta Metall., 1956, vol. 4, pp. 650-54.
48. L. F. Sokiryanskii, D. V. Ignatov, A. Ya. Shinyaev, I. V. Bogolyubova, V. V. Latsh, and M. S. Model: Titanovye Splavy Nov. Tekh., Mater. Nauch.-Tekh. Soveshch., 1966 (pub. 1968), pp. 201-10 (Ed. N. P. Sazhin, Izd. "Nauka": Moscow, USSR), from Chemical Abstracts, 1969, vol. 71, no. 8, 83986r.
49. O. N. Carlson, F. S. Schmidt, and R. R. Lichtenberg: Metall. Trans. A, 1975, vol. 6A, pp. 725-31.

50. R. J. Wasilewski and G. L. Kehl: *J. Inst. of Met.*, 1954-55, vol. 83, pp. 94-104.
51. E. W. Collings: *The Physical Metallurgy of Titanium Alloys*, ASM, Metals Park, OH, 1980, p. 204.
52. S. G. Fedotov, M. G. Chudinov, and K. M. Konstantinov: *Phys. Met. Metallogr*, 1969, vol. 27, pp. 111-14.
53. K. Inoue, Y. Iijima, and K. Hirano: *Titanium '80 Science and Technology*, H. Kimura and O. Izumi, eds., TMS-AIME, 1980, pp. 569-576.
54. A. E. Pontau and D. Lazarus: *Phys. Rev. B*, 1979, vol. 19, pp. 4027-37.
55. J. Unnam, R. N. Shenoy, and R. K. Clark: *Oxid. of Metals*, 1986, vol. 26, pp. 231-52.
56. R. N. Shenoy, J. Unnam, and R. K. Clark: *Oxid. of Metals*, 1986, vol. 26, pp. 105-24.
57. D. J. Derry, D. G. Lees, and J. M. Calvert: *Proc. Brit. Ceram. Soc.*, 1971, no. 19, pp. 77-83.
58. R. Haul and G. Dümberg: *J. Phys. Chem. Solids*, 1965, vol. 26, pp. 1-10.
59. T. B. Gruenwald and G. Gorden: *J. Inorg. Nucl. Chem.*, 1971, vol. 33, pp. 1151-55.

A15 Compound Deformation and Secondary Slip in V_3Si

ROGER N. WRIGHT and KATHLEEN A. BOK

The plastic deformation of A15 compounds has been the subject of a number of investigations. Cold working is possible only under high hydrostatic pressure, and Nb_3Sn, V_3Si, and V_3Ga polycrystals have been cold worked under hydrostatic pressures in the 1790 to 6000 MPa range.[1,2,3] Hot deformation has been more widely evaluated, starting with the work of Greiner and Buehler in 1962.[4] V_3Si single crystal deformation has been studied in the 1200 to 1800 °C range,[4-10] and V_3Ga polycrystal deformation has recently been evaluated in the range from 1000 to 1300 °C.[11,12] The hot deformation of Nb_3Sn polycrystals has been extensively studied in the 1150 to 1650 °C range.[12-15]

The hot deformation stress-strain rate-temperature relationships are largely those of "power law creep", with activation energies for creep roughly in the 400 to 500 kJ/mol range.[11,13,14] Grain size refinement increases flow stress in the power law creep regime.[14] The hot deformed A15 compounds display polygonized dislocation structures.[7,8,9,16] Studies of hot worked V_3Si have noted $\{100\}\langle 010\rangle$ slip systems,[5,6,8,9] and dislocations with cube direction Burgers vectors have been observed.[8,9,17] The creep rate in V_3Si is felt to depend on dislocation climb and the diffusion of V and Si.[8,9,10]

It has been noted that the observed slip systems are inadequate to explain the polycrystalline ductility.[6] There are only three independent $\{100\}\langle 010\rangle$ slip systems, and the observed polycrystalline ductility requires additional modes of microplasticity. In this context etch pit evalua-

tions of plastically deformed V_3Si single crystals and polycrystals have been undertaken.

Slip in V_3Si single crystals and polycrystals was studied using the etch pitting technique of Levinstein *et al.*[5] The materials were obtained from Bell Laboratories, Murray Hill, New Jersey. The single crystals had been compression tested to a plastic strain of about 7 pct at 1300, 1395, 1500, and 1600 °C, as reported by Mahajan *et al.*[6] The compression axis was [110], with crystal plasticity dictating tension in the [1$\bar{1}$0] direction and no plastic strain in the [001] direction. Thus, examination of a (100) plane section should reveal screw or mixed dislocation etch pits corresponding to (010)[100] glide. The specimen orientations were confirmed with standard Laue back reflection technique. The nominal (100) plane section normal was within 6 to 8 deg of the [100] crystallographic direction. The (100) plane sections were metallographically polished, finishing with 0.3 μm alumina in chromic acid. The etch pitting was accomplished with a solution of fifteen parts concentrated hydrofluoric acid and four parts 30 pct hydrogen peroxide. Dislocation etch pits were most easily developed in the specimen plastically deformed at 1300 °C, and no etch pits could be detected in the specimen plastically deformed at 1600 °C. Representative micrographs of the (100) plane sections are shown as Figures 1 and 2.

Polycrystalline V_3Si material was annealed for 168 hours at 1080 °C in argon. The grain size was on the order of 1 mm. A 2.56 mm diameter by 5.15 mm long cylinder was compressed to a plastic strain of about 5 pct at 1300 °C, with a strain rate of about 1.7×10^{-4} s^{-1}. The flow stress was approximately 120 MPa, in reasonable agreement with the flow curves and yield behavior observed by Mahajan *et al.*[6] A micrograph of a sectioned and etched specimen is shown in Figure 3.

The etch pit arrays in Figures 1 and 2 clearly reveal the (010)[100] slip mode and present evidence of noncubic cross slip. Krämer[9] has observed that screw dislocation populations are very low compared to edge and mixed (45 deg) dislocations in hot deformed V_3Si single crystals. The low density of screw dislocations is attributed to relatively high mobility and the possibility of cubic plane cross slip. This may explain the difficulty in observing dislocations on the (100) section plane for [110] direction compression at the higher deformation temperatures. Moreover, many of the dislocations revealed on the (100) section plane may be
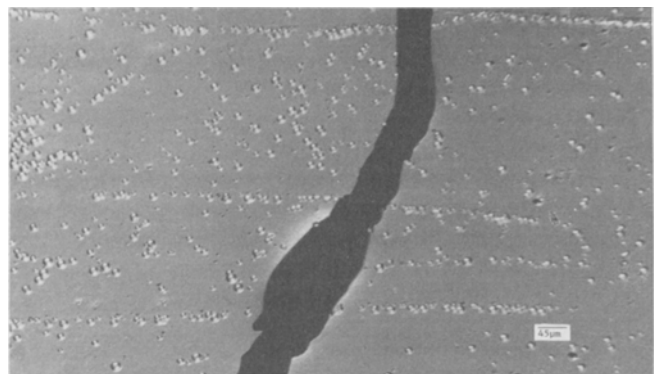

Fig. 1 — Etched screw or mixed character dislocations on a (100) plane section of a V_3Si single crystal deformed at 1300 °C. Horizontal arrays are on (010) glide planes. Black area is a crack in the metallographic specimen.

ROGER N. WRIGHT is Professor and Executive Officer, Rensselaer Polytechnic Institute, Materials Engineering Department, 110 8th Street, Troy, NY 12180-3590. KATHLEEN A. BOK is Process Manager, Procter & Gamble Paper Products, Manufacturing Division, Mehoopany, PA 18629.

Manuscript submitted June 11, 1987.